

Evaluation of a collisional radiative model for electron temperature determination in hydrogen plasma

Cite as: Rev. Sci. Instrum. **93**, 093503 (2022); <https://doi.org/10.1063/5.0101676>
Submitted: 02 June 2022 • Accepted: 29 July 2022 • Published Online: 09 September 2022

 S. P. Vinoth,  E. S. Evans,  C. P. S. Swanson, et al.



View Online



Export Citation



CrossMark



Use the Optimal Technology for All Vacuum Requirements

PFEIFFER VACUUM



Evaluation of a collisional radiative model for electron temperature determination in hydrogen plasma

Cite as: Rev. Sci. Instrum. 93, 093503 (2022); doi: 10.1063/5.0101676

Submitted: 2 June 2022 • Accepted: 29 July 2022 •

Published Online: 9 September 2022



View Online



Export Citation



CrossMark

S. P. Vinoth,^{1,2,a)}  E. S. Evans,¹  C. P. S. Swanson,¹  E. Palmerduca,¹ and S. A. Cohen¹ 

AFFILIATIONS

¹Princeton Plasma Physics Laboratory, Princeton University, Princeton, New Jersey 08543, USA

²Princeton Fusion Systems, Plainsboro, New Jersey 08536, USA

Note: This paper is part of the Special Topic on Proceedings of the 24th Topical Conference on High-Temperature Plasma Diagnostics.

^{a)}**Author to whom correspondence should be addressed:** spunjabi@pppl.gov

ABSTRACT

A collisional-radiative (CR) model that extracts the electron temperature, T_e , of hydrogen plasmas from Balmer-line-ratio measurements is examined for the plasma electron density, n_e , and T_e ranges of 10^{10} – 10^{15} cm⁻³ and 5–500 eV, respectively. The CR code, developed and implemented in Python, has a forward component that computes the densities of excited states up to $n = 15$ as functions of T_e , n_e , and the molecular-to-atomic neutral ratio $r(\text{H}_2/\text{H})$. The backward component provides n_e and $r(\text{H}_2/\text{H})$ as functions of the Balmer ratios to predict the T_e . The model assumes Maxwellian electrons. The density profiles of the electrons and of the molecular and atomic hydrogen neutrals are shown to be of great importance, as is the accuracy of the line-ratio measurement method.

Published under an exclusive license by AIP Publishing. <https://doi.org/10.1063/5.0101676>

I. INTRODUCTION

Collisional-radiative (CR) models^{1,2} are utilized for studying the population distribution of atoms and molecules over their excited vibronic and ionized states, giving information about the relative importance of the different populating and depopulating processes. CR models are at the basis of many plasma diagnostics in the contexts of plasma processing and fusion research. Key parameters³ are electron density (n_e), velocity distribution,^{1,4} and molecular and atomic densities.

CR models for inert gases are relatively straightforward, there being only one species of neutrals. Sasaki *et al.*⁵ measured He-I line ratios in helium plasma to investigate the electron temperature (T_e) and n_e in NAGDIS-I (Nagoya University Divertor Simulator). Bogaerts and Gijbels⁶ used a CR model for argon glow discharges, employing a Monte Carlo model to calculate the electron energy distribution. Balmer-line series are also used to obtain particle and power balances and T_e and n_e measurements in the divertors of fusion research devices.^{7,8}

Hydrogen, being a molecule, is more complex. Johnson and Hinnov⁹ developed a CR model for hydrogen but only considered

the atomic species. Since then, other CR models for the hydrogen atom have been presented, e.g., Ref. 10. Guzman *et al.*¹¹ updated the ADAS¹² tools for CR modeling to include hydrogen molecules.

The CR model that we have developed¹³ can provide T_e for a mixture of molecular (n_{H_2}) and atomic neutrals. This paper shows that knowledge of n_e , n_{H} , and n_{H_2} profiles is essential to extract T_e . Only Maxwellian distributions are considered herein. Importantly, the measured H⁰ density¹⁴ in our fusion research device, the Princeton Field Reversed Configuration (PFRC-2), is of order 10^{11} cm⁻³ and constant in radius while that of H₂ is $\sim 20\times$ higher at the plasma edge and about $10\times$ lower in the plasma core.

II. CR MODEL

In CR models, the densities of the various excited states of a specific atom or ion are expressed as functions of a number of relevant parameters, usually the ground-state density, T_e , and n_e . We constructed in Python a forward component CR model for hydrogen plasma based on Eq. (1). The first and the third terms represent collisional excitation or de-excitation into and out of state i , respectively; the second and fourth terms represent the radiative decay into

and out of state i , respectively; the fifth term represents the ionization of state i ; the sixth term gives the ground-state atomic-hydrogen excitation to state i ; and the last term is used for population-of-state based on molecular dissociation. Negligible recombination occurs in the warm ($T_e > 5$ eV), relatively tenuous ($n_e < 10^{14}$ cm $^{-3}$), high heating-power density PFRC-2 plasmas that are the central focus of our study,

$$\begin{aligned} \frac{dn(i)}{dt} = & \left(n_e \sum_{k \neq i} n(k) \langle \sigma v \rangle_{k \rightarrow i} + \sum_{k > i} A_{k \rightarrow i} n(k) \right) \\ & - \left(n_e \sum_{i \neq k} n(i) \langle \sigma v \rangle_{i \rightarrow k} + \sum_{k < i} A_{i \rightarrow k} n(i) \right) \\ & - n_e n(i) \langle \sigma v \rangle_{i \rightarrow \text{ion}} + n_{\text{H}} n_e \langle \sigma v \rangle_{\text{H} \rightarrow i} \\ & + m_{\text{H}_2} n_e \langle \sigma v \rangle_{\text{H}_2 \rightarrow i}, \end{aligned} \quad (1)$$

where $n(i)$ is the density of the excited state i , $\langle \sigma v \rangle$'s are the Maxwellian-averaged electron-impact reaction rate coefficients, and A 's are the Einstein coefficients. The electron-impact rate coefficients for hydrogen are incorporated from Johnson,¹⁵ Vriens and Smeets,¹⁶ and Sawada *et al.*¹⁷ (Ion-neutral collisions proceed at far slower rates hence are not included.)

The emission-line intensity ratios of the Balmer lines are generated for the n_e range 10^{10} – 10^{15} cm $^{-3}$ and T_e from 5 to 500 eV. The Balmer-line ratios depend strongly on the ratio of molecular to

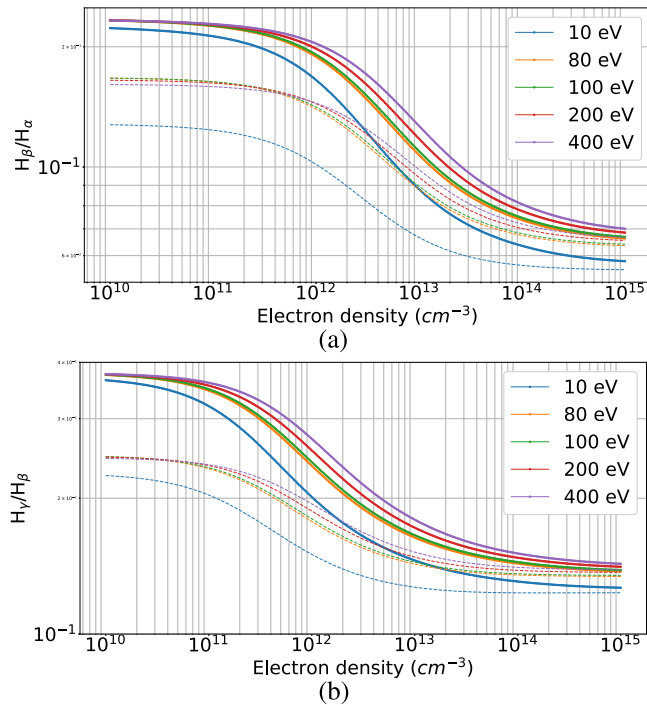


FIG. 1. Two Balmer-line ratios as functions of n_e . (a) Balmer-line ratio H_β/H_α vs n_e for five T_e 's for atomic neutrals (H^0 : solid lines) and molecular neutrals (H_2 : dotted lines). (b) Balmer-line ratio H_γ/H_β vs n_e for five T_e 's for atomic neutrals (H^0 : solid lines) and molecular neutrals (H_2 : dotted lines).

atomic hydrogen densities; see Fig. 1. (The H_α line brightness produced by electron-impact dissociative excitation of H_2 is $\sim 5\times$ less than that caused by electron-impact excitation of H .) The densities of up to $n = 15$ excited states of hydrogen atoms, molecules, or molecular ions are expressed as a function of T_e , n_e , and $r(\text{H}_2/\text{H})$.² The H_β/H_α intensity ratio vs n_e for various T_e are shown in Fig. 1(a) for both pure H and pure H_2 neutrals and those for H_γ/H_β are in Fig. 1(b).

Because the Balmer transitions are of low energy, ~ 2 eV, the change in line ratios becomes increasingly smaller as T_e rises, as seen in Fig. 1.

A. CR model tends to coronal equilibrium (CE) model

A coronal equilibrium (CE) model is appropriate at low density where collisional de-excitation is unimportant. Figure 1 indicates that this occurs for $n_e \lesssim 10^{11}$ cm $^{-3}$. In CE, the fundamental approximations are that all upward atomic transitions are (electron) collisional and all downward transitions are radiative by spontaneous emission.

The upper limit on n_e for a CE model to be applicable can be found by balancing collisional de-excitation and radiative decay. At low density, Eq. (1) becomes

$$\frac{dn(i)}{dt} = n_e n(1) \langle \sigma v \rangle_{1 \rightarrow i} - \left(\sum_{j < i} A_{i \rightarrow j} n(j) \right) + n_e n_{\text{H}_2} \langle \sigma v \rangle_{\text{H}_2 \rightarrow i}. \quad (2)$$

For the $n = 5$ state, and similarly for the $n = 3$ and 4 states, the left-side term in Eq. (3) is the collisional de-excitation rate and the right-side term is the radiative decay rate

$$\begin{aligned} n_e \sum_{5 > i} \langle \sigma v \rangle_{5 \rightarrow i} & \ll \sum_{5 > i} A_{5 \rightarrow i}, \\ n_e & \ll \frac{\sum_{5 > i} A_{5 \rightarrow i}}{\sum_{5 > i} \langle \sigma v \rangle_{5 \rightarrow i}}, \end{aligned} \quad (3)$$

$$n_e < n_{\text{cutoff}},$$

where

$$n_{\text{cutoff}} = \frac{\sum_{5 > i} A_{5 \rightarrow i}}{\sum_{5 > i} \langle \sigma v \rangle_{5 \rightarrow i}}. \quad (4)$$

Figure 2 provides the electron density when the collisional de-excitation rate is 0.1 of the radiative decay rate for $2 < T_e < 50$ eV,

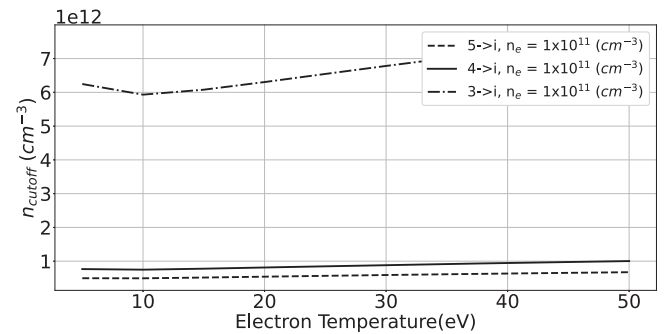


FIG. 2. n_{cutoff} vs T_e for three excited states of H^0 .

a somewhat higher transition density between CR and CE than implied by Fig. 1.

III. SENSITIVITY OF LINE RATIO

A. Sensitivity to T_e

Comparing the Balmer-line ratio for H_2 neutrals at $T_e = 100$ eV to that at 120 eV (see Fig. 1) shows very small differences: the changes in the ratios are $\Delta(H_\beta/H_\alpha) = 0.7\%$ and $\Delta(H_\gamma/H_\beta) = 0.5\%$ for the n_e range $7 \times 10^{11-12} \text{ cm}^{-3}$. The Balmer-line ratios for H_β/H_α and H_γ/H_β vs T_e are shown in Fig. 3 at $n_e = 10^{12} \text{ cm}^{-3}$. For $\Delta T_e/T_e = \pm 10\%$ at $T_e = 100$ eV, the required accuracy for a plasma with only atomic neutrals is $\Delta(H_\beta/H_\alpha) = 0.9\%$. Below $T_e = 25$ eV, about $10\times$ less accuracy is needed in the measured H_β/H_α .

At somewhat higher density, $n_e \sim 10^{13} \text{ cm}^{-3}$, an accuracy of $\pm 1\%$ in H_β/H_α , and an accuracy of $\pm 10\%$ in H_γ/H_β are required for a $\pm 10\%$ accuracy when T_e near 100 eV.

B. Sensitivity to n_e

The sensitivity of the Balmer-line ratio to n_e was evaluated at 100 eV (see Fig. 4). The difference in the Balmer ratio for H_2 neutrals in the range $n_e = (1-10) \times 10^{12} \text{ cm}^{-3}$ shows that $\Delta(H_\beta/H_\alpha) = -42\%$ while for H neutrals, $\Delta(H_\beta/H_\alpha) = -50\%$.

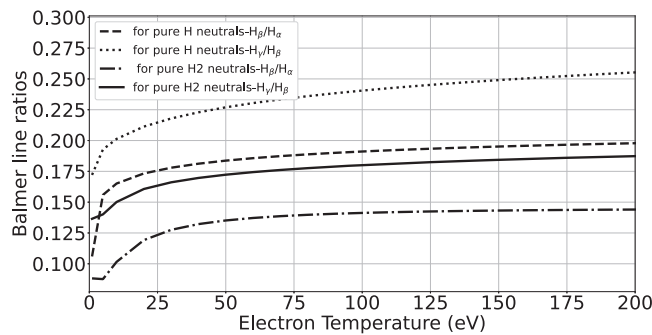


FIG. 3. Balmer line ratios vs T_e at $n_e = 10^{12} \text{ cm}^{-3}$.

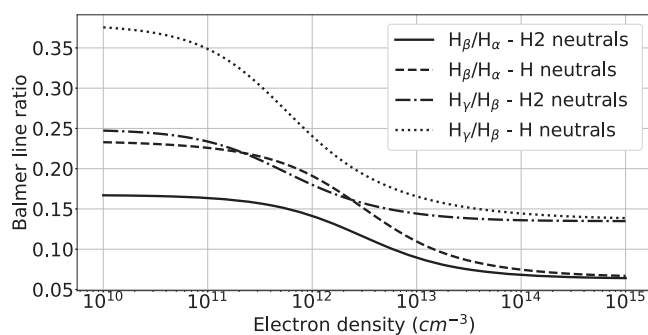


FIG. 4. Balmer line ratio vs n_e at $T_e = 100$ eV.

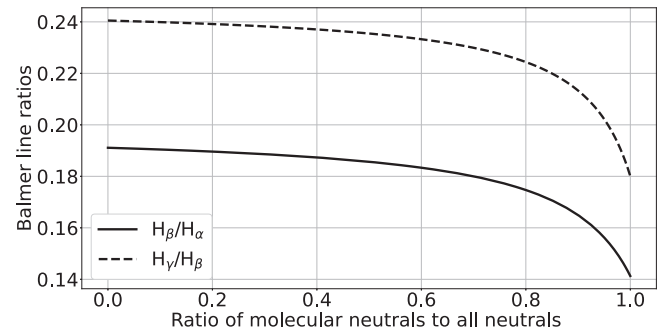


FIG. 5. Balmer-line ratios vs molecular-to-all-neutral hydrogen densities at $T_e = 100$ eV and $n_e = 10^{12} \text{ cm}^{-3}$.

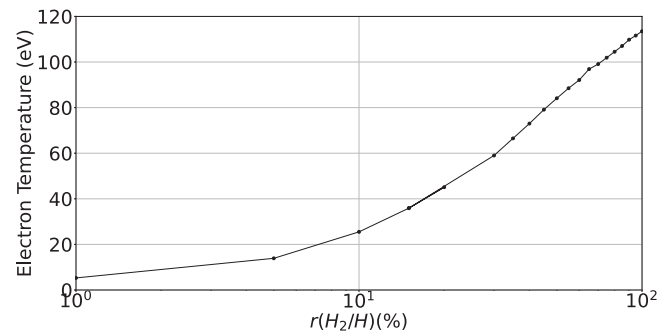


FIG. 6. Extracted T_e for $H_\beta/H_\alpha = 0.13$, $n_e = 10^{12} \text{ cm}^{-3}$, and different percentages of molecular to all neutral densities.

C. Sensitivity to neutral population densities

The Balmer-line ratio is highly sensitive to the ratio of the molecular to the sum of all neutral densities (Fig. 5). The Balmer-line ratio difference at $r(H_2/(H + H_2))$ of 0.99 and 0.9 was $\Delta(H_\beta/H_\alpha) \sim \Delta(H_\gamma/H_\beta) \sim 14\%$. This density-ratio range is representative of that in the PFRC-2 edge plasma.

The effect of the neutral density ratio on the extracted T_e is shown in Fig. 6 for $H_\beta/H_\alpha = 0.13$. At a 1% concentration of H_2 , the inferred T_e is 6 eV, while at 90%, it is 110 eV. Knowledge of the neutral densities is clearly essential to accurately determine T_e . Two-photon absorption laser induced fluorescence (TALIF)¹⁴ can provide the atomic neutral density profile. At present, the H_2 profile is calculated for the PFRC-2 using the DEGAS neutral transport code. It shows the H_2/H ratio changes from 1:10 in the PFRC-2 plasma's core to 10:1 at its edge. Use of this data also requires knowledge of the plasma density profile because the Balmer line ratios are line averages. Spectrometer observations through chords having different tangency radii will reduce this uncertainty.

IV. DETERMINATION OF LINE RATIO

This section describes the methods that we have evaluated for obtaining the strength of a spectral line when computing Balmer line ratios for PFRC-2.

Pulsed, odd-parity rotating magnetic field (RMF) antennas create a hydrogen plasma in the center cell with the goal of inducing

a field-reversal configuration (FRC). Hydrogen line intensities are measured using a Model 9590212 Ocean FX-Spectrometer, set at $150\ \mu\text{s}$ integration time. The PFRC-2 was operated at vacuum central magnetic field of 140 G, absorbed power $\sim 16\ \text{kW}$, initial fill pressure of 0.3 mTorr, and pulse width of 7 ms. Several methods were compared for finding the Balmer-line ratios. Prior to these tests, the spectrometer sensitivity vs wavelength was measured with two integrating spheres, sources of nominally black-body-like radiation.

A. Counts under the peak

In this method, the line intensity is determined by summing all the counts “under” the peak, as shown in Fig. 7. These data were produced in less than three minutes of clock time by accumulating photons over 159 shots at $t = 1.08 \pm 0.075\ \text{ms}$ of the 7 ms width pulses. Near the H_β wavelength, the spectrometer dispersion was about 6 pixels/nm. 17 pixels to either side of the maximum have been included; outside this range, the counts per pixel are lesser than 1/500 of the peak value and are the region used for background subtraction.

B. Gaussian fit

In this approach, a Gaussian fit is applied to the data obtained from the spectrometer (see Fig. 8). The area under the Gaussian is used to obtain the line intensity. The Gaussian is chosen to match the

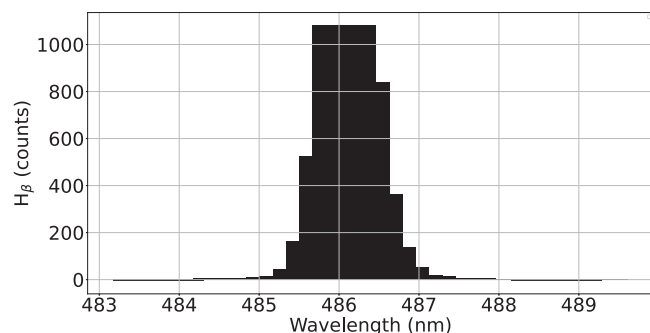


FIG. 7. Illustration of summing the counts under a spectral peak (for H_β) to obtain the intensity.

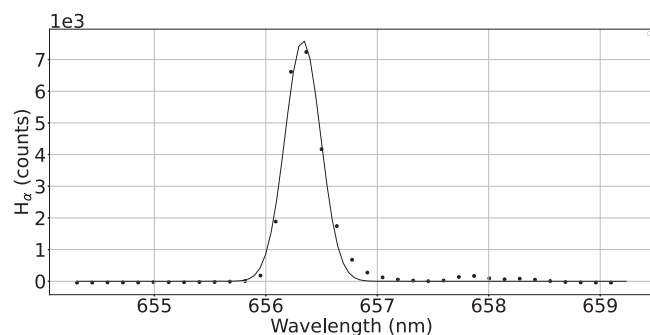


FIG. 8. Gaussian fit for the H_α line.

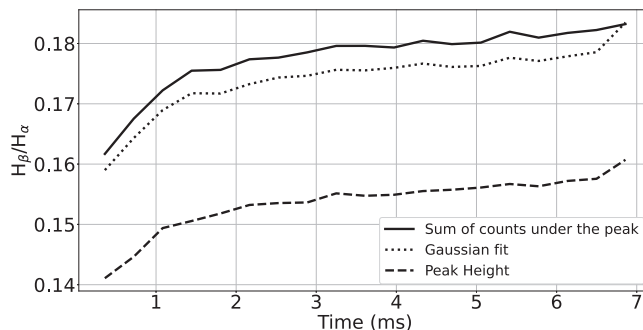


FIG. 9. Balmer-line ratios produced via each of the three methods in Sec. IV for the same 159 PFRC-2 discharges. During each of these discharges, the plasma density fell from 3×10^{12} to $8 \times 10^{11}\ \text{cm}^{-3}$ in the first ms then stayed constant.

peak height and half-width; however, the fit is poorer on the line’s wings. In this wavelength range, the line of a laser also shows similar asymmetry, leading us to attribute the non-Gaussian shape to an instrumental effect of the Ocean FX-spectrometer.

C. Peak height

In this approach, the pixel with the greatest number of counts near the line of interest provides the peak height from which the intensity is computed. The peak-height method differs from the Gaussian method because the peak height of a narrow line depends on where its central wavelength falls relative to the pixel boundaries in the spectrometer’s detector. A narrow line centered on one pixel will have one peak height, but centered between two pixels, and the same line would have a smaller peak height.

D. Comparison

The Balmer-line ratios vs time for the mentioned experimental condition are shown in Fig. 9. Each method yields a different line ratio; thus, different values for T_e when those line ratios are used with the CR model. The Gaussian and area-under-peak methods differ by about 5%, while the peak-amplitude method is lower by 25%. Consideration of the physics issues leads us to conclude that the most accurate method for determining the line ratios is to sum the counts under the peak, as it accounts for factors, particularly the spectrometer dispersion, that affect the distribution of counts vs wavelength.

V. AN ELECTRON TEMPERATURE MEASUREMENT

In consideration of the three aforementioned factors—the measured line ratios, the % of H_2 , defined as $P_c \equiv 100n_{\text{H}_2}/(n_{\text{H}_2} + n_{\text{H}})$, and n_e —we extract estimates of $T_e(t)$. The line ratio statistics provide the error bar, the shaded region in Fig. 10.

The n_e measurement is a line average. For the same profile shape, n_e depends inversely on the separatrix radius. Based on probe data and fast camera observations, we use a separatrix radius of 5 cm. We note, in passing, that, if n_e is known, using two line ratios, e.g., H_β/H_α and H_γ/H_β , can reduce the uncertainty in the value of P_c used to calculate T_e .

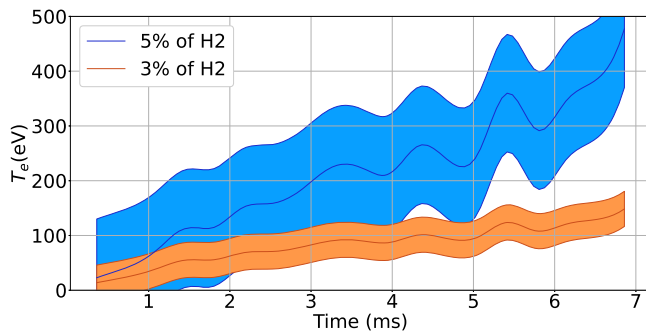


FIG. 10. Extracted $T_e(t)$ for the data in Fig. 9 for two values of P_c . The shaded region represents the statistical error bar.

The P_c value in the core depends on the accuracy of the TALIF measurements and the DEGAS simulations; the latter depends on T_e . The T_e considered in DEGAS span the range 20–100 eV, predicting $5 < P_c < 25\%$. Based on pressure-gauge and TALIF measurements, P_c at the edge exceeds 10. However, the plasma edge n_e is lower, hence the emission dimmer. We do not include the high P_c at the edge in the data analysis, hence provide a conservative estimate of T_e .

Figure 10 shows the extracted $T_e(t)$ for two values of P_c , 3% and 5%. For these PFRC-2 experimental conditions, if P_c is above 10%, this CR model predicts that T_e exceeds 500 eV. The shaded region indicates the $\pm\sigma$ uncertainty due to the Balmer-line ratio statistics. Near the measured plasma line-average density, T_e is approximately proportional to $4/r$ (cm).

The increasing line ratio during the discharge (see Fig. 9) causes the extracted T_e to increase. Figure 10 displays the important feature first noted in Fig. 1: the neutral density ratio, P_c , is critical in extracting T_e . Conversely, if T_e is known via another diagnostic, P_c can be determined. We note that x-ray diagnostics on the PFRC-2, which measure the Bremsstrahlung spectrum above 500 eV, have shown T_e in the range of 100–400 eV. The number of plasma discharges to acquire the x-ray data with the same time resolution was about 30 greater than the Balmer-line-ratio technique described herein.

VI. SUMMARY

A CR model developed for the hydrogen plasma was evaluated. It converts to CE model when n_e is less than 10^{11} cm^{-3} . The CR method is highly sensitive to n_e and its radial profile, and the ratio of molecular to atomic neutrals and their radial profiles. Accurate determination of line intensities, that is, spectrometer calibration, is also crucial for use of the model to extract accurate T_e . First tests of the CR model on the PFRC-2 have been made, including comparisons with other diagnostics. These comparisons are informative as different diagnostics sample different parts of the electron energy distribution function.

ACKNOWLEDGMENTS

This work was supported, in part, by the U.S. Department of Energy under Contract No. DE-AC02-09CH11466, by ARPA-E

Award No. DE-AR0001099 (Princeton Fusion Systems), and by the Princeton Program in Plasma Science and Technology, Princeton University. We are grateful to M. Paluszek and S. J. Thomas for their continued support and B. Berlinger and C. Brunkhorst for excellent technical work.

AUTHOR DECLARATIONS

Conflict of Interest

The authors have no conflicts to disclose.

Author Contributions

S. P. Vinoth: Formal analysis (lead); Software (equal). **E. S. Evans:** Software (equal). **C. P. S. Swanson:** Formal analysis (equal). **E. Palmerduca:** Software (equal). **S. A. Cohen:** Supervision (equal).

DATA AVAILABILITY

The data that support the findings of this study are openly available at <https://dataspace.princeton.edu/handle/88435/dsp01x920g025r>.¹⁸

REFERENCES

- 1 I. H. Hutchinson, "Principles of plasma diagnostics," *Plasma Phys. Controlled Fusion* **44**, 2603 (2002).
- 2 T. Fujimoto, K. Sawada, and K. Takahata, "Ratio of Balmer line intensities resulting from dissociative excitation of molecular hydrogen in an ionizing plasma," *J. Appl. Phys.* **66**, 2315–2319 (1989).
- 3 S. Iordanova and T. Paunskaa, "A collisional radiative model of hydrogen plasmas developed for diagnostic purposes of negative ion sources," *Rev. Sci. Instrum.* **87**, 02B110 (2016).
- 4 M. A. Lieberman and A. J. Lichtenberg, *Principles of Plasma Discharges and Materials Processing* (John Wiley & Sons, 2005).
- 5 S. Sasaki, S. Takamura, S. Watanabe, S. Masuzaki, T. Kato, and K. Kadota, "Helium I line intensity ratios in a plasma for the diagnostics of fusion edge plasmas," *Rev. Sci. Instrum.* **67**, 3521–3529 (1996).
- 6 A. Bogaerts, R. Gijbels, and J. Vlcek, "Collisional-radiative model for an argon glow discharge," *J. Appl. Phys.* **84**, 121–136 (1998).
- 7 K. Verhaegh, B. Lipschultz, B. P. Duval, A. Fil, M. Wensing, C. Bowman, and D. S. Gahle, "Novel inferences of ionisation and recombination for particle/power balance during detached discharges using deuterium Balmer line spectroscopy," *Plasma Phys. Controlled Fusion* **61**, 125018 (2019).
- 8 R. Prakash, T. Pütterich, R. Dux, A. Kallenbach, R. Fischer, and K. Behringer, "Spectroscopic divertor characterization and impurity influx measurements in ASDEX upgrade tokamak," IPP Report No. 10/31, 2006.
- 9 L. C. Johnson and E. Hinnov, "Ionization, recombination, and population of excited levels in hydrogen plasmas," *J. Quant. Spectrosc. Radiat. Transfer* **13**, 333–358 (1973).
- 10 D. Wunderlich, S. Dietrich, and U. Fantz, "Application of a collisional radiative model to atomic hydrogen for diagnostic purposes," *J. Quant. Spectrosc. Radiat. Transfer* **110**, 62–71 (2009).
- 11 F. Guzmán, M. O'Mullane, and H. P. Summers, "ADAS tools for collisional-radiative modelling of molecules," *J. Nucl. Mater.* **438**, S585–S588 (2013).

¹²H. Summers, The ADAS User Manual, version 2.6, <http://www.adas.ac.uk/>, 2004.

¹³S. P. Vinoth *et al.*, “Electron temperature measurement using spectroscopic measurements of Balmer’s ratio in PFRC-II pulsed hydrogen plasmas using collisional radiative model,” in 62nd Annual Meeting of the APS Division of Plasma Physics, 2020, <https://meetings.aps.org/Meeting/DPP20/Session/VP13.2>.

¹⁴A. Dogariu, S. Cohen, E. Evans, S. Vinoth, and C. Swanson, “A diagnostic to measure neutral atom density in RF-heated PFRC-2 plasmas,” *Rev. Sci. Instrum.* (these proceedings) (2022).

¹⁵L. C. Johnson, “Approximations for collisional and radiative transition rates in atomic hydrogen,” *Astrophys. J.* **174**, 227 (1972).

¹⁶L. Vriens and A. H. M. Smeets, “Cross-section and rate formulas for electron-impact ionization, excitation, deexcitation, and total depopulation of excited atoms,” *Phys. Rev. A* **22**, 940 (1980).

¹⁷K. Sawada, K. Eriguchi, and T. Fujimoto, “Hydrogen-atom spectroscopy of the ionizing plasma containing molecular hydrogen: Line intensities and ionization rate,” *J. Appl. Phys.* **73**, 8122–8125 (1993).

¹⁸See <https://dataspace.princeton.edu/handle/88435/dsp01x920g025r> for example for the following paper “Electron heating in 2-D: combining Fermi-Ulam acceleration and magnetic-moment non-adiabaticity in a mirror-configuration plasma” the MATLAB codes used in this paper are found on the same website.